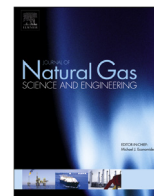




Contents lists available at ScienceDirect

## Journal of Natural Gas Science and Engineering

journal homepage: [www.elsevier.com/locate/jngse](http://www.elsevier.com/locate/jngse)

## Effect of clay and organic matter on nitrogen adsorption specific surface area and cation exchange capacity in shales (mudrocks)

Milad Saidian<sup>\*,1</sup>, Lemuel J. Godinez<sup>2</sup>, Manika Prasad

Colorado School of Mines, USA

### ARTICLE INFO

#### Article history:

Received 13 October 2015  
 Received in revised form  
 23 April 2016  
 Accepted 26 May 2016  
 Available online xxx

#### Keywords:

Cation exchange capacity  
 Specific surface area  
 Organic rich shales  
 Organic matter  
 Thermal maturity

### ABSTRACT

The resistivity log and its conventional application is one of the most important analysis used to find oil and gas saturated intervals. In unconventional oil and gas producing rocks, however, this tool and the consequent technique, is affected by many factors and not considered very reliable. Shale reservoir rocks usually have high total specific surface area (TSSA) due to high clay and total organic content (TOC) and nano-scale pores. Resistivity values are rather low and usually not indicative of reservoir zones in high TSSA rocks. Nitrogen adsorption and cation exchange capacity (CEC) are the common techniques to measure TSSA. Clays and organic matter (OM) affect the measured TSSA using either technique. This effect must be taken into account while calculating water saturation using conventional models. In this paper we investigate the mineralogical and geochemical associations of CEC and TSSA and their effects on resistivity in shale reservoirs.

We studied samples from oil and gas producing reservoirs such as Bakken, Haynesville, European Silurian, Niobrara, and Monterey formations. CEC was measured using Co(III)-hexamine<sup>3+</sup> with the spectrophotometric technique and the equivalent TSSA (CEC-TSSA) was calculated. We also measured the specific surface area using sub-critical Nitrogen gas adsorption technique (N<sub>2</sub>-SSA). Rock mineralogy, organic matter properties and scanning electron microscope (SEM) images were used to further analyze the data.

We find that CEC values are directly correlated with the clay type and content regardless of the OM content or level of thermal maturity. Smectite and illite (when negligible smectite is present) dominate the CEC value in shales. N<sub>2</sub>-SSA correlates with clay content, especially smectite and illite, but is less sensitive to clay type as CEC. This correlation between N<sub>2</sub>-SSA and clay content was observed in Bakken (no organic matter), thermally mature (gas window) Haynesville, and low TOC (<2.67 wt%) Niobrara (oil window) samples. We also find that OM significantly affects N<sub>2</sub>-SSA in two different ways: (1) Blockage of pores and throats by bituminous kerogen, which limits the accessibility of nitrogen to clay surfaces. This effect was observed in thermally immature (oil window) Niobrara (TOC>2.6 wt%) and Monterey shales. (2) Development of nano-scale OM-hosted pores with high surface area mostly for thermally mature (gas window) shales as observed in high TOC (>1.5 wt%) Silurian shales. Correlation with N<sub>2</sub>-SSA and CEC values revealed that the average charge density for most of the shales in this study varies between 3 and 5 e/nm<sup>2</sup> and for some high TOC Niobrara samples can be as high as 32. Relatively higher charge density is due to underestimation of the TSSA by nitrogen adsorption technique. The correlation between SSA/CEC and clay content/type are well studied in the literature. However the results of this study aid in understanding how mineralogy, geological factors, organic matter content and thermal maturity affect this correlation in mud rocks from various reservoirs.

© 2016 Published by Elsevier B.V.

### 1. Introduction

Presence of clays with high specific surface area (SSA) and its effect on resistivity log response has been investigated (for example, Archie, 1942; Waxman and Smits, 1968; Clavier et al., 1984; Revil et al., 1998). Unaccounted excess conductivity due to

\* Corresponding author.

E-mail addresses: [milad.saidian@gmail.com](mailto:milad.saidian@gmail.com) (M. Saidian), [lemuel.godinez@yahoo.com](mailto:lemuel.godinez@yahoo.com) (L.J. Godinez), [mprasad@mines.edu](mailto:mprasad@mines.edu) (M. Prasad).

<sup>1</sup> Now at BP America, USA.

<sup>2</sup> Now at Oasis Petroleum, USA.

clay minerals results in underestimation of hydrocarbon volume in hydrocarbon producing reservoirs (Waxman and Smits, 1968). To evaluate the excess conductivity due to clay minerals, information is required about the number of counterions on clay surfaces, expressed as the cation exchange capacity (CEC) (Clavier et al., 1984). It was shown that the CEC and SSA are linearly correlated for clays (Woodruff and Revil, 2011) and shaly sands (Patchett, 1975; Revil et al., 2013). Therefore, accurate measurements of SSA and CEC as well as an understanding of their control factors are crucial for reliable resistivity log interpretation. The mineral or organic matter surfaces probed depend on the technique used for SSA measurement. For example, gas adsorption with inert gases (such as nitrogen) measures the external specific surface area (ESSA) (Derkowski and Bristow, 2012; Heister, 2014) whereas polar liquid (e.g. ethylene glycol monoethyl ether or EGME) adsorption techniques measure the total specific surface area (TSSA) (Heister, 2014; and Zhu et al., 2014).

Shales have high surface area because of high clay content (Passey et al., 2010) and nano-scale pores that are hosted by organic matter or minerals such as clays (Loucks et al., 2012; Milliken et al., 2013; Kuila et al., 2014). These rocks also have various amount of organic matter with different types and various levels of thermal maturity. Petrophysical and textural properties of the organic matter change as a result of maturation process (Zargari et al., 2013; and Zargari et al., 2015). Both clays and organic matter affect the measured CEC and surface area of shales in different ways. Clays, when present, dominate the measured CEC and SSA of the rock. There is a significant difference between the SSA and CEC of different clays (Table 1). Smectite and illite clays have the highest CEC and SSA and usually dominate the SSA of the clay rich rocks (Ellis, 1987; and Derkowski and Bristow, 2012). The effect of organic matter (OM), however, is more complicated than clay effect. OM can affect the SA measurements in three different ways: (1) Chemical interaction with the investigating fluid that is used for SSA or CEC measurement (Chiou et al., 1993; Derkowski and Bristow, 2012), (2) it can limit the accessibility of the investigating fluid to the surface of the minerals by blocking the pores and throats or coating the clay surfaces themselves (Lang and Kaupenjohann, 2003; Mikutta et al., 2004), (3) Developing nano-scale pores as a result of thermal maturation and diagenesis of the organic matter (Kuila et al., 2014; and Zargari et al., 2015). Chemical interaction and developing nano-scale pores might

**Table 1**

Cation exchange capacity (CEC), nitrogen adsorption specific surface area (N<sub>2</sub>-SSA) and ethylene glycol monoethyl ether total specific surface area (EGME-TSSA) for different clay types and isolated kerogen.

Sample	CEC (meq/100gr)	SSA-N <sub>2</sub> (m <sup>2</sup> /gr)	TSSA-EGME (m <sup>2</sup> /gr)
Smectite <sup>a</sup>	76.1–150 <sup>b–f</sup>	31.13 <sup>i</sup> , 75.9 <sup>j</sup>	400–850 <sup>h,m</sup>
Illite	9–40 <sup>b–d,t,g</sup>	25 <sup>k</sup> , 67.2 <sup>j</sup>	57–118 <sup>h,m</sup>
Chlorite	1 <sup>c</sup>	15 <sup>k</sup>	9–62 <sup>h,m</sup>
Kaolinite	0.9–15 <sup>a–e,h</sup>	11.5 <sup>i</sup> –21 <sup>j</sup>	9–62 <sup>h,m</sup>
Kerogen	<0.5 <sup>h</sup>	5.5–300 <sup>l</sup>	860–921 <sup>h</sup>

<sup>a</sup> Smectite and different types of Montmorillonite are combined.

<sup>b</sup> Wiklander (1964).

<sup>c</sup> Thomas (1976).

<sup>d</sup> Ridge (1983).

<sup>e</sup> Ellis (1987).

<sup>f</sup> Blum and Eberl (2004).

<sup>g</sup> Śródoń (2009).

<sup>h</sup> Derkowski and Bristow (2012).

<sup>i</sup> Kuila and Prasad (2013).

<sup>j</sup> Chiou et al. (1993).

<sup>k</sup> Van Olphen and Fripiat (1979).

<sup>l</sup> Cao et al. (2015).

<sup>m</sup> Revil et al. (2013).

increase the measured CEC and SSA, whereas, the blockage of the pore space and coating of the clay surfaces decrease the measured SSA.

The effects of clay and OM on CEC and SSA are well studied in soils (Chiou et al., 1993; Peinemann et al., 1999; Maček et al., 2013; and Heister, 2014). However, the interactions between OM and clays and their effects on the CEC and SSA in organic-rich sedimentary rocks are largely unknown and more complicated due to diagenetic changes in OM and mineral properties. Controversial results are reported especially on the effect of OM on CEC and SSA. Zhu et al. (2014) report positive and negative correlations between TOC with various textures and morphologies and SSA measured by N<sub>2</sub> and EGME techniques for oil bearing mudrocks from eastern China. In this study, the overestimation of TSSA with the EGME method in presence of OM is neglected Derkowski and Bristow (2012); Keil et al. (1994) and Mayer and Xing (2001) report an increase in TSSA (measured by retention techniques) with increasing OM content in immature and non-altered soils. A similar correlation is reported for black shales from Late Cretaceous black shales of the Deep Ivorian Basin by Kennedy and Wagner (2011) and Kennedy et al. (2002). However, a negative correlation between TOC and SSA was observed by Kuila et al. (2012) for oil window Niobrara samples and by Ding et al. (2013) for muddy source rock and oil shale from the Oligocene Shahejie Formation.

Our literature survey revealed that several factors need to be considered during comparisons of results from different studies or formations: (1) the technique that is used for SSA or CEC measurement and their advantages and limitations, (2) TOC and level of thermal maturity, (3) clay type and content and (4) organic matter texture and distribution. A comprehensive study of the effect of rock composition and organic matter on CEC and SSA for shales considering all these factors is lacking.

In this study we present CEC and SSA data for rock samples from different oil and gas producing shales. We cover a wide range of clay content and type, TOC and thermal maturity and organic matter texture to study the effect of rock composition on the measured CEC and SSA. We also compare the SSA calculated from CEC data and measured by nitrogen adsorption technique (N<sub>2</sub>-SSA) and provide insights on application of these values for resistivity log interpretation.

## 2. Materials

In this section we briefly describe the dominant mineralogy, thermal maturity, organic matter type, and organic matter content for the samples used for this study (Fig. 1). The details of each sample set have been presented by Kuila (2013) and Saidian et al. (2016) (Haynesville, Niobrara, and Eastern European Silurian), Rivera et al., 2014 and Godinez, 2013 (Monterey), and Saidian and Prasad, 2015 (Bakken). The key properties of kerogen and clay for all sample sets are given in Table 2.

### 2.1. Bakken

Samples from Middle Bakken and Three Forks formations were carbonate rich, mainly dolomite with moderate amount of clay and quartzo-feldspic. The clay was mainly illite and no organic content was present (Fig. 1a).

### 2.2. Haynesville

Haynesville samples were clay-rich with moderate amounts of quartzo-feldspathic constituents and carbonate (Fig. 1b).

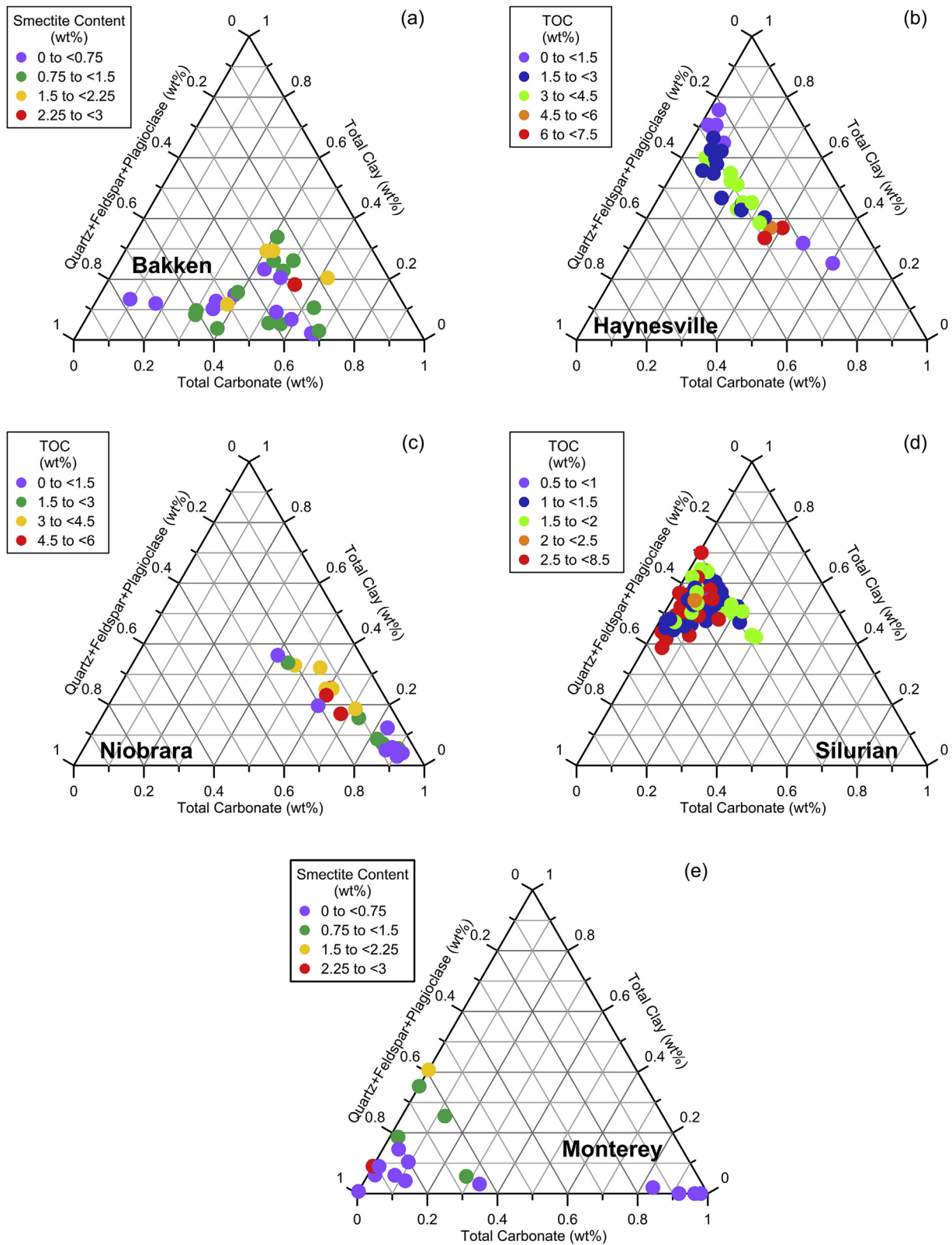


**Fig. 1.** Mineralogy of the (a) Bakken, (b) Haynesville, (c) Niobrara and (d) Silurian (e) Monterey samples. Bakken and Monterey samples are color coded with smectite content and Haynesville, Silurian and Niobrara are color coded with TOC. Note that Bakken samples contain no organic matter and the TOC for Monterey samples is not available.

**Table 2**  
Kerogen and clay properties for all sample sets. The values in bracket are average values for the property.

Sample set	TOC wt%	HI	T <sub>max</sub> °C	I-S wt%	S in I-S wt%
Bakken	0	NA	NA	2–29 (13)	0–51(<10)
Haynesville	0.5–6.3 (2.8)	19–57 (36)	Up to 542	20–60 (40)	0–9(<5)
Silurian	1–8(2.4)	<9	NA	24–50(39)	0–20(<5)
Niobrara	0.1–5.3(2.3)	120–387(306)	417–443(436)	3–35(16.3)	14–95(35)
Monterey	1–5 <sup>a</sup>	184–473(374) <sup>a</sup>	438 <sup>a</sup>	0–40(10)	0–32(6)

<sup>a</sup> Data are measured for adjacent samples from the same well. TOC = Total Organic Carbon, HI = Hydrogen Index, I-S = mixed layer illite-smectite, S in I-S = % Smectite in I-S.

### 2.3. European Silurian

European Silurian samples (henceforth referred as Silurian) contained up to 52 wt% quartz and up to 57 wt% clay which is mostly illite (Fig. 1c).

### 2.4. Niobrara

Marl and chalk samples came from the Berthoud Field, Larimer County, CO, USA, from both the Fort Hays limestone and the overlying Smoky Hill members of the Niobrara formation. Samples were calcite-rich rocks with moderate amounts of clay, quartz and pyrite (Fig. 1d).

### 2.5. Monterey

Core samples were taken from the western flank of the southern San Joaquin Basin in California. The samples were quartz phase porcelanites containing moderate amounts of clay and pyrite (Fig. 1e).

## 3. Methods

In this section, we briefly describe the pretreatments, and methods for Nitrogen adsorption and CEC measurement techniques. Techniques such as X-Ray Diffraction (XRD), Rock Eval and Scanning Electron Microscopy (SEM) were utilized to characterize the mineralogy, organic content and nano-scale structure of the samples, respectively. Table 3 lists the number of samples from each formation that were used in different experiments.

### 3.1. Sub-critical nitrogen gas adsorption (N<sub>2</sub>)

The method has been described in detail elsewhere (Sing et al., 1985) and its adaptation for mudrocks is detailed in (Kuila, 2013). The main advantage of this technique is assessing nano-scale pores (1.7–200 nm). However since the samples are dried prior to the experiment, the nitrogen molecules do not penetrate the clay interlayers and the external surface area (referred as N<sub>2</sub>-SSA henceforth) of the clays is measured.

### 3.2. Cation exchange capacity (CEC)

Cation Exchange Capacity was measured using the Co(III)-

**Table 3**  
Number of samples from each formation that were used in different experiments. N<sub>2</sub>-SSA stands for nitrogen adsorption specific surface area, CEC=Cation Exchange Capacity, XRD = X-Ray Diffraction.

Experiment	Bakken	Haynesville	Silurian	Niobrara	Monterey
N <sub>2</sub> -SSA	12	22	19	22	16
CEC	12	34	80	21	18
XRD	12	34	80	22	18
Rock Eval	NA	34	80	22	NA

hexamine<sup>3+</sup> with the spectrophotometric technique according to Bardon et al. (1993). The lower limit of CEC detected by this method is normally 0.5 meq/100 gr and the standard deviation is about 1.4 meq/100 gr (Derkowski and Bristow, 2012).

## 4. Results

The goal of our study was to examine the sensitivity of the surface area and CEC to mineral composition and OM. To achieve this goal, we examined samples with a wide range of clay content and type, kerogen content, thermal maturity and type. The samples belonged to various oil and gas producing formations: predominantly carbonate with no organic matter (Bakken), predominantly clay (Haynesville); mineral mixture (Silurian), and predominantly carbonate (Niobrara), predominantly quartz (Monterey). In the following, we present CEC and N<sub>2</sub>-SA results for each formation and investigate the main control factors.

### 4.1. Bakken

Cross plots of CEC and N<sub>2</sub>-SSA with mixed layer illite-smectite for Bakken samples are shown in Fig. 2a and b, respectively. From Fig. 2 we observe that: CEC shows a linear correlation with mixed layer illite-smectite for low smectite content (<10% in mixed illite-smectite layer) samples (Fig. 2a). N<sub>2</sub>-SSA shows linear correlation with mixed layer illite-smectite with high correlation coefficient (R<sup>2</sup> = 0.85) (Fig. 2b). Illite is the dominant clay type (Table 2); other minerals appear uncorrelated with CEC and N<sub>2</sub>-SSA. Using CEC = 20 meq/100 gr for pure illite (Table 1) the measured CEC for Bakken samples with illite content of 2–29 wt% should not exceed approximately 5.4 meq/100 gr which matches the measured data. The linear fit shown in Fig. 2b yields N<sub>2</sub>-SSA of 33.84 m<sup>2</sup>/g for 100% mixed layer illite-smectite which matches the ranges reported in Table 1. Similarly, CEC of 100% mixed layer illite-smectite for low smectite samples is 10.49 meq/100 g.

### 4.2. Haynesville

Cross plots of CEC and N<sub>2</sub>-SSA with mixed layer illite-smectite, color-coded by TOC, for Haynesville samples are shown in Fig. 3a and b, respectively. We make the following observations: Both CEC and N<sub>2</sub>-SSA have linear correlation with mixed layer illite-smectite. CEC shows a better correlation (R<sup>2</sup> = 0.80) compared to N<sub>2</sub>-SSA (R<sup>2</sup> = 0.63). Note that the number of N<sub>2</sub>-SSA measurements is less than CEC measurements. Although there are different clay types in Haynesville samples, Illite is the dominant clay type (Table 2). Abundance of Illite is mainly due to high thermal maturity (gas window). Other minerals or TOC show no correlation with CEC and N<sub>2</sub>-SSA. Assuming an approximate CEC value of 20 meq/100 gr for pure illite (Table 1) the measured CEC for Haynesville samples with illite content of 19–60 wt% should not exceed approximately 12 meq/100 gr which matches the measured data. The linear fit in Fig. 3b shows N<sub>2</sub>-SSA of 42.24 m<sup>2</sup>/gr for 100% mixed layer illite-smectite which matches the ranges reported in Table 1.

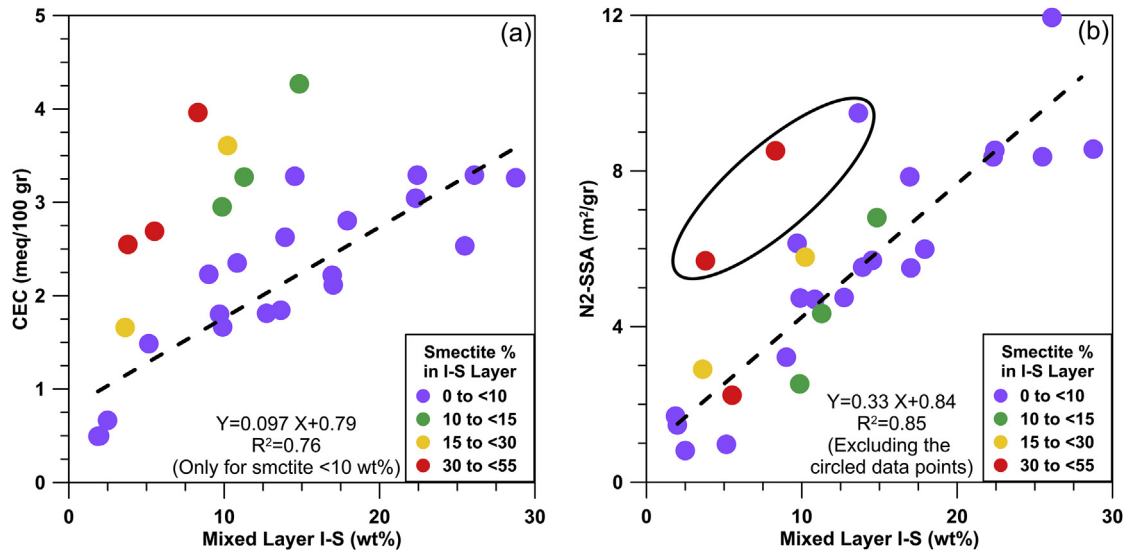


**Fig. 2.** The cross plot of (a) CEC and (b) N<sub>2</sub>-SSA with mixed layer illite-smectite content for Bakken samples. Linear correlation was found between mixed layer illite-smectite and CEC of low smectite (illite rich) (a) N<sub>2</sub>-SSa (b).

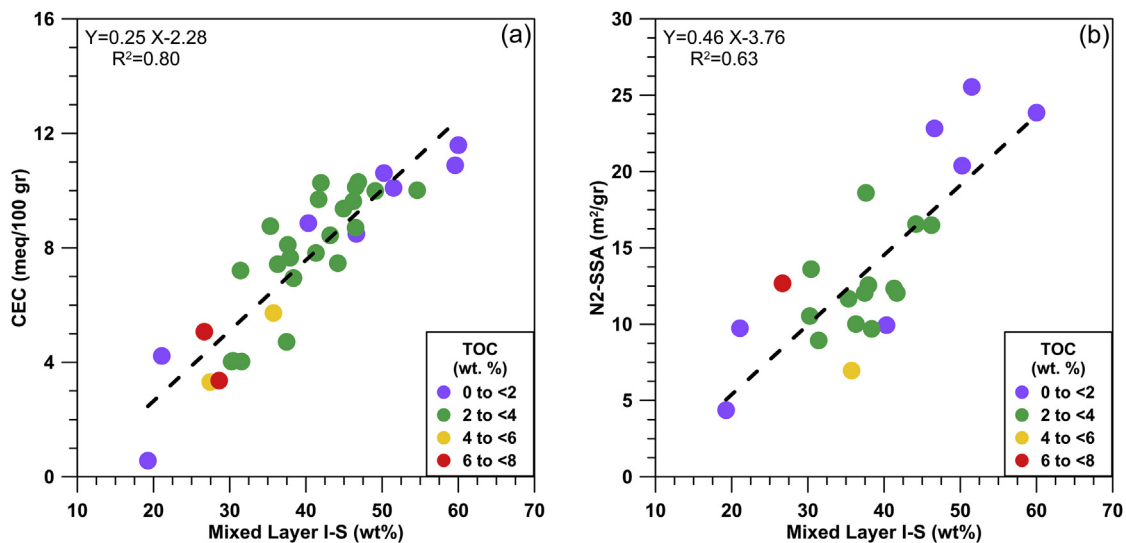


**Fig. 3.** The cross plot of (a) CEC and (b) N<sub>2</sub>-SSA with mixed layer illite-smectite content for Haynesville samples color coded by TOC. Note that the amount of smectite is negligible. Both CEC and N<sub>2</sub>-SSA have linear correlation with mixed layer illite-smectite. CEC shows a better correlation ( $R^2 = 0.80$ ) compared to N<sub>2</sub>-SSA ( $R^2 = 0.63$ ). Note that the number of N<sub>2</sub>-SSA measurements is less than CEC measurements.

#### 4.3. Silurian

Saidian et al. (2016) showed that in the same Silurian samples the TOC and clay content affect the nitrogen adsorption pore size distribution for low and high TOC samples. We plotted the Silurian CEC and N<sub>2</sub>-SSA data against mixed layer illite-smectite based on a TOC cutoff of 1.5 wt% in Fig. 4 and Fig. 5. We make the following observations: Illite is the dominant clay in Silurian samples (Table 2) mainly due to high thermal maturity (gas window). Both CEC and N<sub>2</sub>-SSA for low TOC samples (<1.5 wt%) show a linear correlation with mixed layer illite-smectite content (Note that the number of N<sub>2</sub>-SSA measurements is less than CEC measurements). For high TOC samples, neither CEC nor N<sub>2</sub>-SSA show any correlation with mixed layer illite-smectite. Although N<sub>2</sub>-SSA appears to have a weak negative correlation with mixed layer illite-smectite (Fig. 5b), we believe this correlation is a result of scatter of the data. It is expected to have a positive correlation between N<sub>2</sub>-SSA and mixed

layer illite-smectite. The N<sub>2</sub>-SSA seems to increase by increasing TOC in high TOC (>1.5 wt%) samples. Assuming an approximate CEC value of 20 meq/100 gr for pure illite (Table 1) the measured CEC for Silurian samples with illite content of 23–50 wt% should not exceed approximately 10 meq/100 gr which matches the majority of the measured data. Assuming an approximate N<sub>2</sub>-SSA value of 40 m<sup>2</sup>/gr for pure illite (Table 1 and values calculated for pure illite in Bakken and Haynesville Samples) the measured N<sub>2</sub>-SSA for Bakken samples with illite content of 23–50 wt% should not exceed approximately 20 m<sup>2</sup>/gr which matches the measured data.

#### 4.4. Niobrara

Niobrara mixed layer illite-smectite contains significant amount of smectite clay compared to other sample sets (Table 2). Smectite clay dominates the CEC response (Table 1), when present, so we plotted the CEC in Niobrara versus smectite content in Fig. 6a. N<sub>2</sub>-

SSA for smectite is in the same range as illite (Table 1) so we showed the cross plot of N<sub>2</sub>-SSA and mixed layer illite-smectite in Fig. 6b. The following observations can be made for Fig. 6: CEC of Niobrara samples shows a good correlation ( $R^2 = 0.91$ ) with the smectite content of the samples (Fig. 6a). N<sub>2</sub>-SSA is linearly correlated with mixed layer illite-smectite content for Low TOC Chalk samples (<2.6 wt%) with a very high correlation coefficient ( $R^2 = 0.99$ ) (Fig. 6b). High TOC marl samples (>2.6 wt%) show lower N<sub>2</sub>-SSA compared to low TOC chalk samples (<2.6 wt%) (Fig. 6b). Assuming an approximate CEC value of 100 meq/100 gr for pure smectite (Table 1) the measured CEC for Niobrara samples with smectite content of zero to 11 wt% should not exceed approximately 11 meq/100 gr. Higher measured CEC for these samples (up to 14 meq/100 gr) is due to the extra CEC of the illite (38–99% of the mixed layer illite-smectite is illite) (Fig. 6a). The linear fit in Fig. 6b shows N<sub>2</sub>-SSA of 43 m<sup>2</sup>/gr for 100% mixed layer illite-smectite in low TOC (<2.6 wt%) samples which matches the ranges reported in Table 1.

#### 4.5. Monterey

Similar to Niobrara samples, Smectite is the most abundant clay type in Monterey samples (Table 2). We plotted CEC versus smectite content and N<sub>2</sub>-SSA versus mixed layer illite-smectite in Fig. 7a and b, respectively. TOC data were not available for these samples. Based on Fig. 7 the following observations can be made: CEC shows a linear correlation with smectite content. Whereas, N<sub>2</sub>-SSA does not show any correlation with mixed layer illite-smectite. Assuming an approximate CEC value of 100 meq/100 gr for pure smectite (Table 1) the measured CEC for Monterey samples with smectite content of zero to 2.88 wt% should not exceed approximately 2.88 meq/100 gr (Fig. 7a). Higher measured CEC for these samples (up to 14 meq/100 gr) is due to the extra CEC of the illite (67.7–99.9% of the mixed layer illite-smectite is illite). Assuming an approximate N<sub>2</sub>-SSA value of 40 m<sup>2</sup>/gr for pure illite (Table 1) the measured N<sub>2</sub>-SSA for Monterey samples with mixed layer illite-smectite content of 0–39 wt% should not exceed approximately 15.6 m<sup>2</sup>/gr. The measured surface areas for Monterey samples are much lower than expected value.

## 5. Discussion

In this comparative study we analyze the CEC and N<sub>2</sub>-SSA differences for each sample set honoring the mineralogical and geochemical properties of each formation. Samples were chosen from different formations; Middle Bakken and Three Forks (Bakken) formations are oil producing with no organic matter, Haynesville and Silurian formations are highly mature (gas window) with low hydrogen index (Table 2). The Niobrara and Monterey samples are less mature (oil window) with high hydrogen index (Table 2). In this section we first discuss the effect of rock mineralogy, (especially clay content and type) and organic content and maturity on measured CEC and N<sub>2</sub>-SSA values. Then we compare the surface areas calculated using both techniques.

### 5.1. Effect of rock composition on CEC

CEC values can be estimated by taking an arithmetic average of individual clay CEC values (Patchett, 1975; Pezard, 1990; Revil et al., 1998; and Derkowski and Bristow, 2012). We validated the measured CEC values in the results section for all sample sets. The linear correlation between CEC and clays presented in Figs. 2a–7a also confirms that CEC strongly depends on the clay type and content. For comparison we plotted CEC data versus mixed layer illite-smectite for all samples sets (Fig. 8). Niobrara samples show higher CEC values compared to the rest of sample sets due to presence of smectite in mixed layer illite-smectite clay. Monterey samples show higher scatter compared to Niobrara samples because of low smectite content. As shown in results section, the CEC data for this sample set is also affected by the illite content. Bakken and Haynesville CEC (Fig. 8) show linear correlation with mixed layer illite-smectite for a wide range of clay content. Silurian samples, despite being thermally mature and illite-rich, show lower CEC values (Fig. 8). Underestimation of CEC for the Silurian samples is explained by examining microstructural differences in SEM images for Bakken (Fig. 9), Haynesville (Fig. 10), and Silurian (Fig. 11) samples.

SEM images for illite-rich shales such as Bakken (Fig. 9) and Haynesville (Fig. 10) samples show that the surface of the illite flakes is not covered with organic matter. This has been observed for Haynesville samples with different clay and organic matter

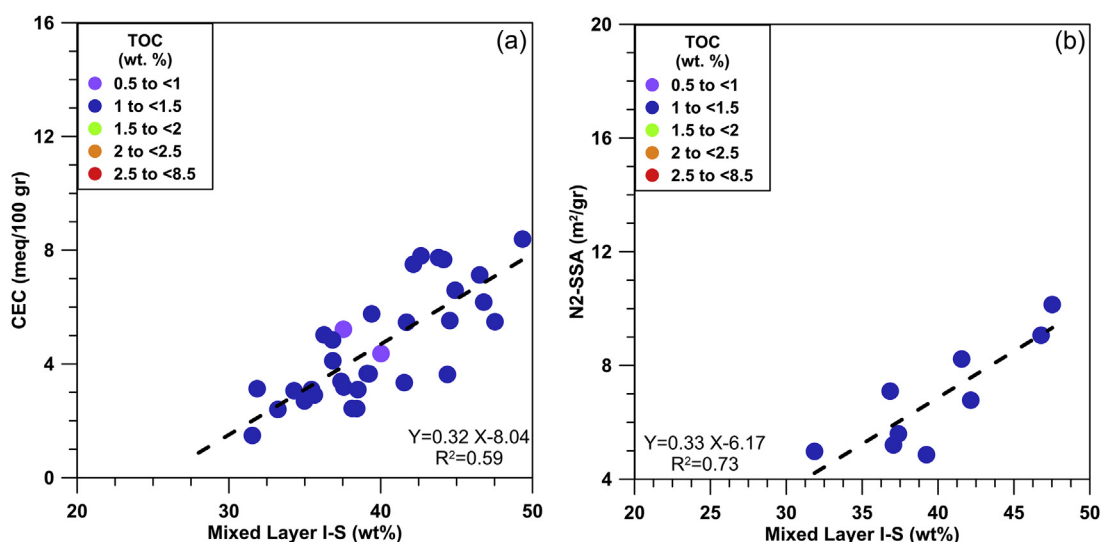
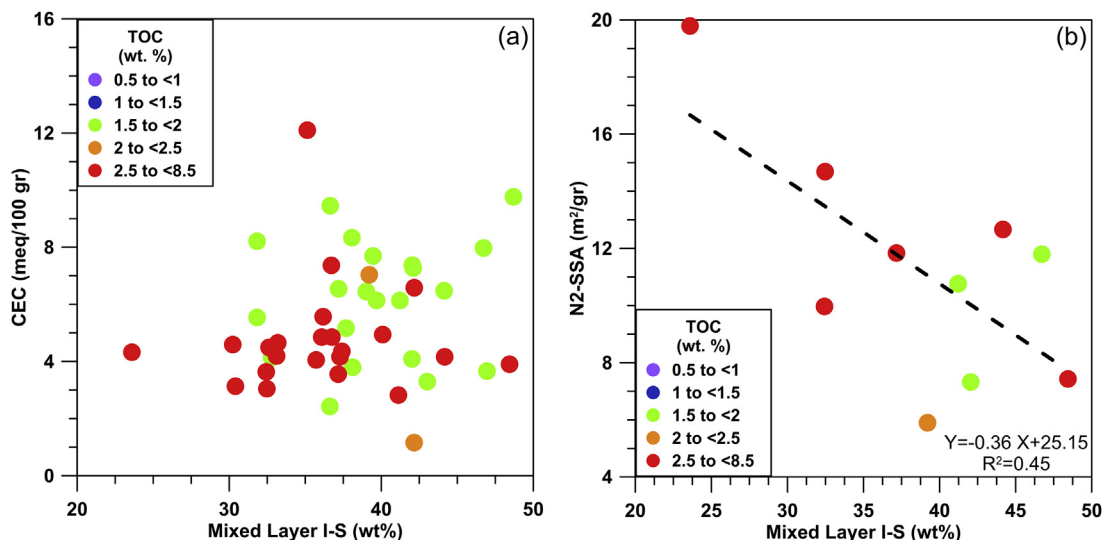
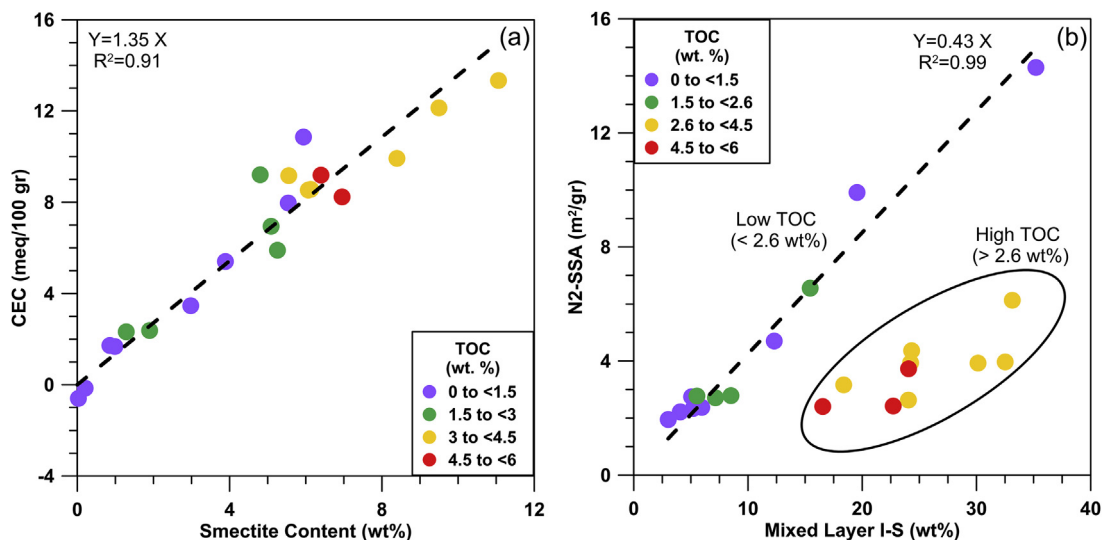


Fig. 4. Cross plot of (a) CEC and (b) N<sub>2</sub>-SSA with mixed layer illite-smectite color coded with TOC for low TOC (<1.5 wt%) Silurian samples. CEC and N<sub>2</sub>-SSA for Low TOC (<1.5 wt%) samples show a linear correlation with the mixed layer-illite smectite content which is similar to Bakken and Haynesville sample sets.



**Fig. 5.** Cross plot of (a) CEC and (b) N2-SSA with mixed layer illite-smectite color coded with TOC for high TOC (>1.5 wt%) Silurian samples. CEC and N2-SSA for Low TOC (<1.5 wt%) samples do not show any correlation with mixed layer illite-smectite content or with TOC (not shown here).



**Fig. 6.** Cross plot of (a) CEC and smectite content and (b) N2-SSA and mixed layer illite-smectite for Niobrara samples. CEC of Niobrara samples shows a good correlation ( $R^2 = 0.91$ ) with the smectite content (a). N2-SSA is linearly correlated with mixed layer illite-smectite content for Low TOC samples (<2.6 wt%) with a very high correlation coefficient ( $R^2 = 0.99$ ) (b). High TOC samples (>2.6 wt%) show lower N2-SSA compared to low TOC samples (<2.6 wt%) (b).

content (for more SEM images see Saidian et al., 2016). SEM images for Silurian samples (Fig. 11) show the effect of compaction on closure of pores. The underestimation of CEC (Fig. 7) is due to minimum exposure of minerals, especially clays. In the following we will discuss the effect of TOC on the exposure of the illite clay.

Based on the mineralogy of the samples (Fig. 1), CEC of the samples (Fig. 7) and the CEC of pure clays and kerogen (Table 1), we concluded that smectite and illite (when smectite is minimal or not present) dominate the CEC value of the samples.

The other rock component that might affect the measured CEC and N2-SSA is the organic matter (OM). Since retention surface area measurement techniques were not used in this study, we focus on other effects of organic matter: the pore and throat blockage and development of nano-scale OM hosted pores. Derkowski and Bristow (2012) showed that in sedimentary OM, the CEC values lie below detection limits, regardless of thermal maturity (Table 1). Thus, the presence of nano-scale OM-hosted pores does not

contribute to the CEC values. Also, since CEC measurements are performed by hydrating the rock, the pore and throat blockage do not limit the accessibility of the ions to probe the clay inter layers. The linear correlation between smectite or illite content regardless of TOC and thermal maturity, confirms the findings of Derkowski and Bristow (2012). Exceptions to these observations might be found in samples from highly compacted formations.

### 5.2. Effect of rock composition on N2-SSA

In contrast to CEC, N2-SSA values cannot be estimated by arithmetic average of pure clay N2-SSA. The N2 technique evaluates the external surface area of the clays. As shown in Table 1, the N2-SSA values do not vary as much as CEC values do within a single data set. Fig. 12 shows the N2-SSA data for all sample sets, plotted against mixed layer illite-smectite clay content. In this figure, Bakken, Haynesville and low TOC (>2.6 wt) chalk Niobrara samples

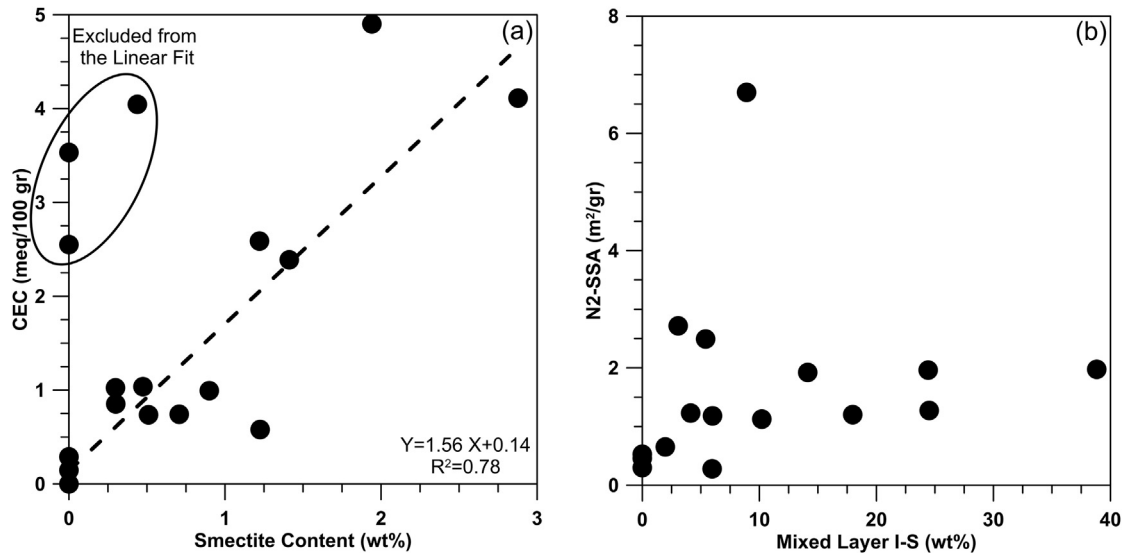


Fig. 7. Cross plot of (a) CEC and smectite content and (b) N<sub>2</sub>-SSA and mixed layer illite-smectite content for Monterey samples. TOC data were not available for these sample sets. CEC is linearly correlated with smectite clay and N<sub>2</sub> do not show any correlation with mixed layer illite-smectite. Not that the points circled in (a) were not included in the fit.

show similar correlation with mixed layer illite-smectite content. Monterey, high TOC Niobrara and low TOC Silurian demonstrate underestimated N<sub>2</sub>-SSA. High TOC Silurian samples generally have higher N<sub>2</sub>-SSA compared to low TOC Silurian samples.

The effect of clay content on N<sub>2</sub>-SSA data cannot be interpreted without considering the effect of organic matter. Our results show that the effect of organic matter on N<sub>2</sub>-SSA is more profound than CEC. Bakken with no organic matter, Haynesville (gas window) with organic matter up to 6.5 wt% and low TOC (<2.6 wt%) Niobrara (oil window) demonstrates similar linear correlation with mixed layer illite-smectite. Similar to Bakken and Haynesville, SEM image for Low TOC Niobrara (Fig. 13a) shows exposure of the mixed layer

illite-smectite minerals for nitrogen adsorption measurements. Based on the linear fit in Fig. 12, 100% mixed layer illite-smectite N<sub>2</sub>-SSA is 35.88 m<sup>2</sup>/gr which is in the range that is reported in the literature (Table 1). The smectite content does not affect the correlation since both illite and smectite have similar N<sub>2</sub>-SSA (Table 1).

Linear correlation in Fig. 12 shows that in low organic matter samples or when the organic matter does not coat the clay surfaces or fill up the mineral pores, regardless of the thermal maturity, the N<sub>2</sub>-SSA is correlated with mixed layer illite-smectite content.

The underestimation of N<sub>2</sub>-SSA for Silurian, high TOC Niobrara and Monterey samples is due to two different OM effects; blockage by bituminous kerogen and compaction of pores. The data plotted from Kuila et al. (2014) (Fig. 14) shows that removing organic matter from organic rich samples with high hydrogen index (>150, oil window) such as Niobrara and Monterey increases the N<sub>2</sub>-SSA. This confirms the blockage of pores by bituminous kerogen in oil window samples.

SEM image for high TOC Niobrara (Fig. 13) shows how OM blocks or coats the clay minerals. This blockage does not affect the CEC data (Fig. 8), but it is detrimental to N<sub>2</sub>-SSA measurements (Fig. 12).

In Silurian samples the compaction closed the pores and caused creep of thermally mature kerogen in the pores and coating of the clay surfaces (Fig. 11). The consistent reduction in both CEC and N<sub>2</sub>-SSA confirms this observation. However, presence of OM-hosted pores in high TOC Silurian samples to some extent compensated the reduction in surface area. This justifies the higher N<sub>2</sub>-SSA for high TOC Silurian samples (Fig. 12) and the correlation that was observed in (Fig. 5a) for TOC and N<sub>2</sub>-SSA of these samples.

Our results show that in oil window samples pore blockage by bituminous kerogen does not affect the CEC, but it reduces the N<sub>2</sub>-SSA. However, developing nano-scale pores in gas window increases the measured N<sub>2</sub>-SSA and has no effect (negligible effect) on CEC values.

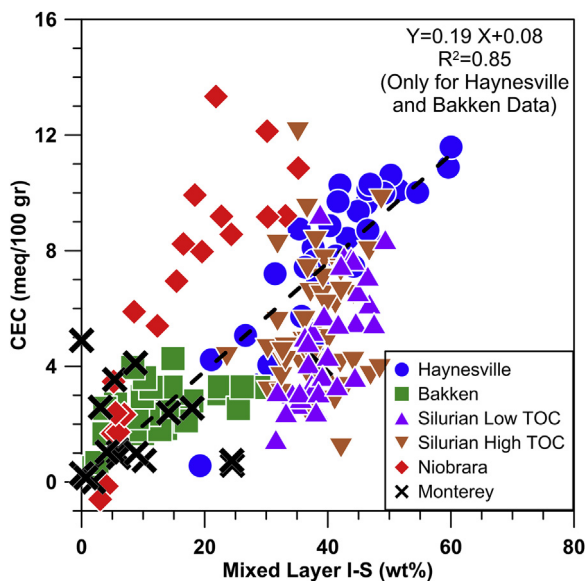
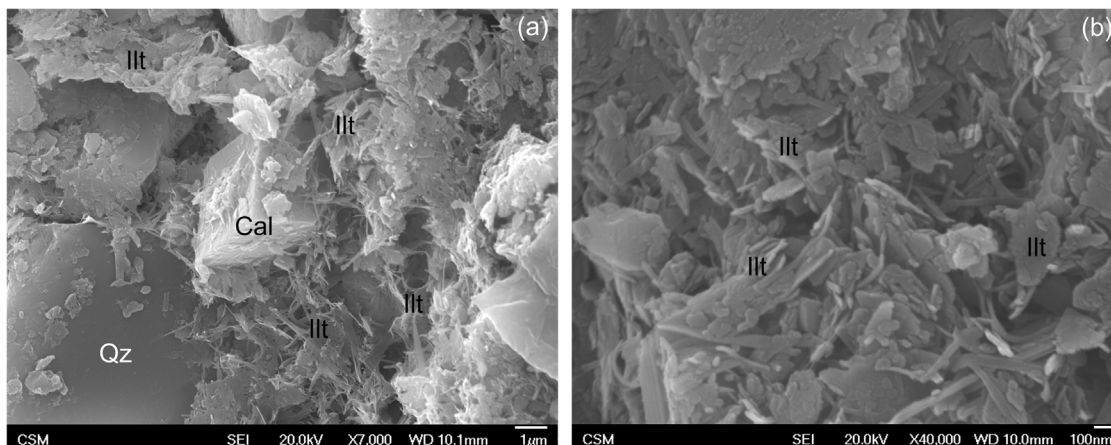


Fig. 8. Cross plot of CEC and mixed layer illite-smectite for all sample sets. Niobrara and Monterey data show higher CEC values compared to the rest of sample sets due to presence of smectite in mixed layer illite-smectite clay. Bakken and Haynesville CEC show linear correlation with mixed layer illite-smectite for a wide range of clay content. Silurian samples, despite being thermally over mature and illite-rich, show lower CEC values compared to Bakken and Haynesville samples.

### 5.3. Correlation between CEC-TSSA and N<sub>2</sub>-SSA

The CEC values can be converted to smectite equivalent assuming a theoretical CEC of 95–100 meq/100 gr for the smectitic surfaces of illite-smectite and common pure smectites (Środoń,



**Fig. 9.** SEM images (Backscattered Electron Images) for Bakken samples at (a) 7000 and (b) 40000 magnifications showing the illite clays distributed in the rock. Illite is the dominant clay which is distributed in the rock matrix and is fully exposed for CEC and N<sub>2</sub>-SSA measurements. There is negligible amount of other clays such as chlorite (up to 3.4 wt % with an average value of 1.3 wt%) in these samples. Qz = Quartz, Cal = Calcite, Ill = Illite.

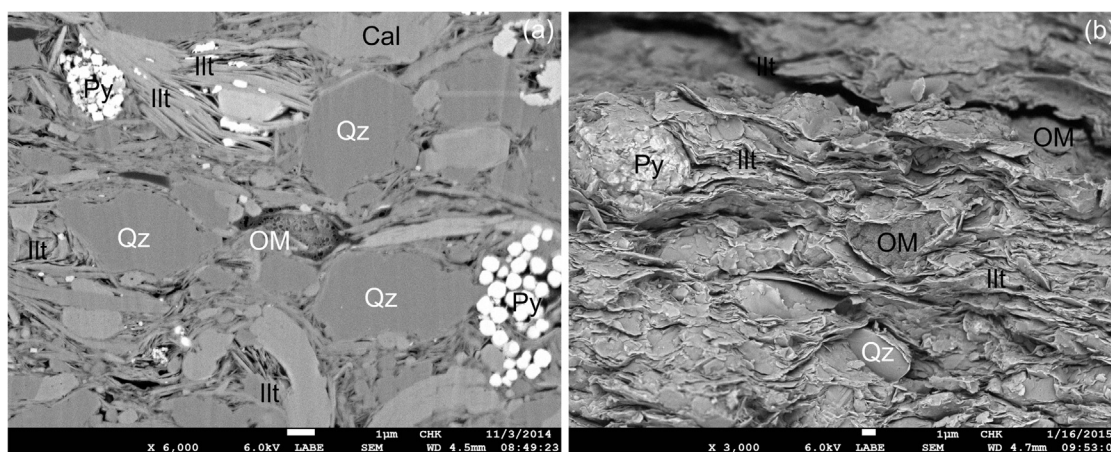


**Fig. 10.** SEM images (Backscattered Electron Images) for (a) ion beam polished and (b) unpolished Haynesville samples. In these samples despite the presence of TOC and other clays such as chlorite, illite is the mineral that dominates the measured CEC and N<sub>2</sub>-SSA. Both images show that the surface of the illite flakes are fully exposed and not covered with organic matter. Qz = Quartz, Cal = Calcite, Py = Pyrite, Ill = Illite, OM = Organic Matter.

2009). The CEC equivalent total specific surface area (CEC-TSSA) was calculated from the “smectite equivalent” values assuming a theoretical surface area of 800 m<sup>2</sup>/g of pure smectite (Derkowski

and Bristow, 2012; and Revil et al., 2013). The surface area was also measured by N<sub>2</sub> technique. However drying the samples at 200 °C under vacuum prior to the N<sub>2</sub>-SSA measurements

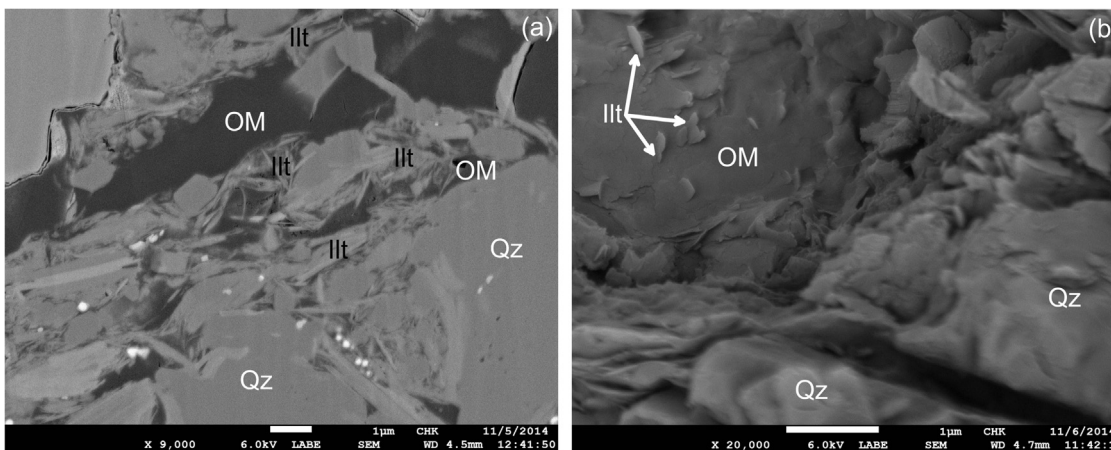


**Fig. 11.** SEM images (Backscattered Electron Images) for (a) ion beam polished and (b) unpolished for high TOC (>1.5 wt%) Silurian samples. The effect of compaction on pore closure and creep of organic matter into pore space is observed. In high TOC Silurian samples the clay flakes are coated with organic matter and are less exposed for CEC and N<sub>2</sub>-SSA. Qz = Quartz, Ill = Illite, OM = Organic Matter.

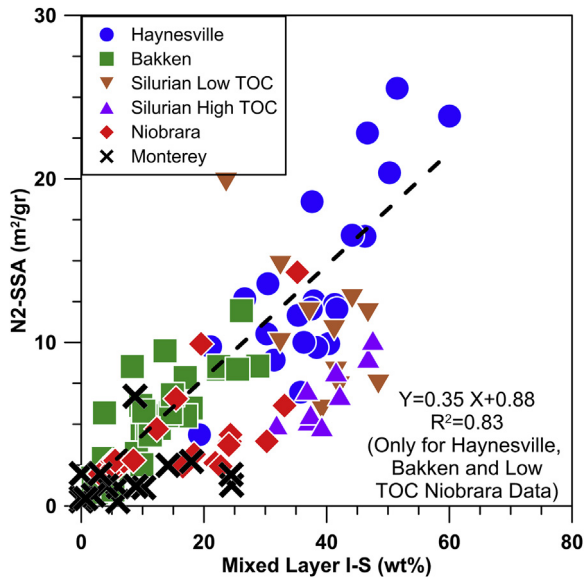


**Fig. 12.** The N<sub>2</sub>-SSA data for all sample sets, plotted against mixed layer illite-smectite clay content. Bakken, Haynesville and low TOC (<2.6 wt) chalk Niobrara samples show similar correlation with mixed layer illite-smectite content. Monterey, high TOC Niobrara and low TOC Silurian demonstrate underestimated N<sub>2</sub>-SSA. High TOC Silurian samples generally have higher N<sub>2</sub>-SSA compared to low TOC Silurian samples.

evaporates the adsorbed water to the clay surfaces and collapses the clay layers. As a result the nitrogen molecules only access the external surface of the clays (Derkowski and Bristow, 2012). This limited accessibility of the nitrogen molecules results in an underestimation of the surface area measured by N<sub>2</sub> technique compared to other techniques such as the CEC equivalent surface area.

The simple conversion of CEC values to CEC-TSSA, allows for the estimation of total specific surface area and can then be plotted to compare to the BET specific surface area obtained from nitrogen gas adsorption (Fig. 15). This figure shows that the specific surface area values obtained by nitrogen gas adsorption are an underestimation. It is recommended that BET specific surface areas obtained by nitrogen gas adsorption not be used as the absolute values of total specific surface area but rather used as qualitative parameters to compare the pore structure of various mudrocks. The shaly sand

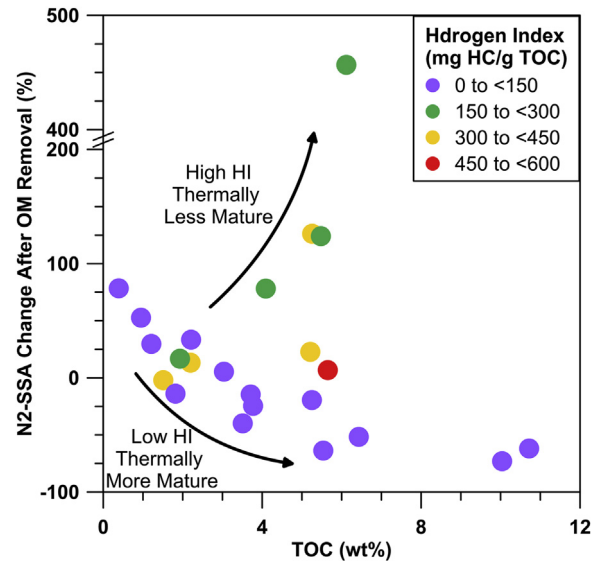


**Fig. 14.** Data plotted from Kuila et al. (2014) showing the change in N<sub>2</sub>-SSA after organic matter removal. Low hydrogen index (HI) samples (<150), which are thermally mature samples, show decrease in N<sub>2</sub>-SSA after OM removal. This change in surface area is due to removal of nano-scale organic-hosted pores in thermally mature samples. High HI samples (>150) show an increase in N<sub>2</sub>-SSA after removal of organic matter. Increase in N<sub>2</sub>-SSA is due to exposing the clay flakes that were coated by organic matter prior to bleaching process.

data from Patchett (1975) correspond to an average surface charge density of 1.5 e/nm<sup>2</sup>, which is equivalent to 0.24 c/m<sup>2</sup>. Woodruff and Revil (2011) have estimated a surface charge density of 0.32 c/m<sup>2</sup> for shaly sands, while Środoń (2009) estimated a 0.42 c/m<sup>2</sup> surface charge density for clay bearing rocks (Revil et al., 1998; and Derkowski and Bristow, 2012). The charge density for organic rich shales and Bakken in this study is in the 3–5 e/nm<sup>2</sup> which is equivalent to 0.48–0.80 c/m<sup>2</sup> and some of the Niobrara samples show a charge density of 32 e/nm<sup>2</sup> which is equivalent to 5.13 c/m<sup>2</sup>.

These charge density values are overestimated and are not necessarily aligned with what should technically be expected from shaly sands. This overestimation is due to low surface areas measured with nitrogen gas adsorption. Since N<sub>2</sub>-SSA is only external surface area, a much higher surface charge density is needed to accommodate the CEC range measured. This is a reason

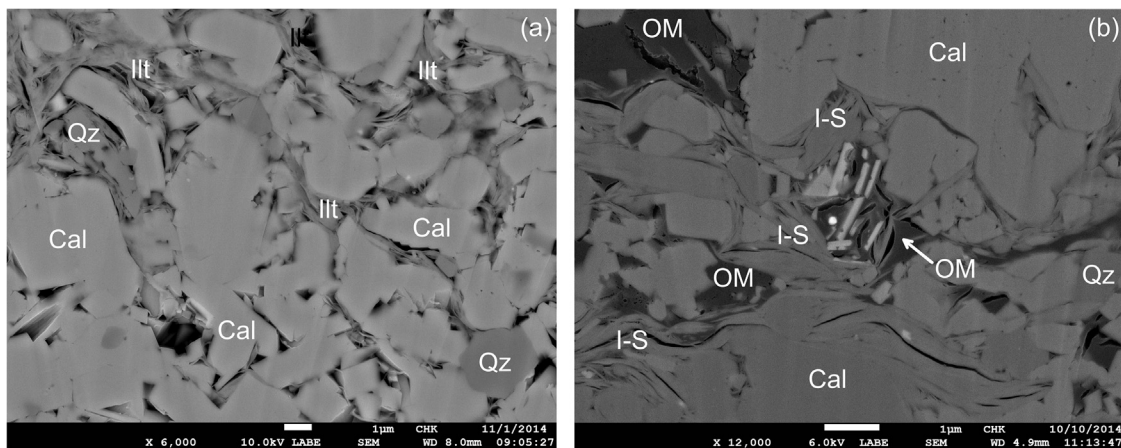


**Fig. 13.** SEM images (Backscattered Electron Images) for (a) low TOC (<2.6 wt% chalk) and (b) high TOC (>2.6 wt% marl) Niobrara samples. Mixed layer illite-smectite layers are more exposed in low TOC chalk samples. The OM in marl (b) block or coat the clay surfaces and limits the accessibility of nitrogen molecules. Qz = Quartz, I-S = Mixed Layer Illite-Smectite, Cal = Calcite, OM = Organic Matter.

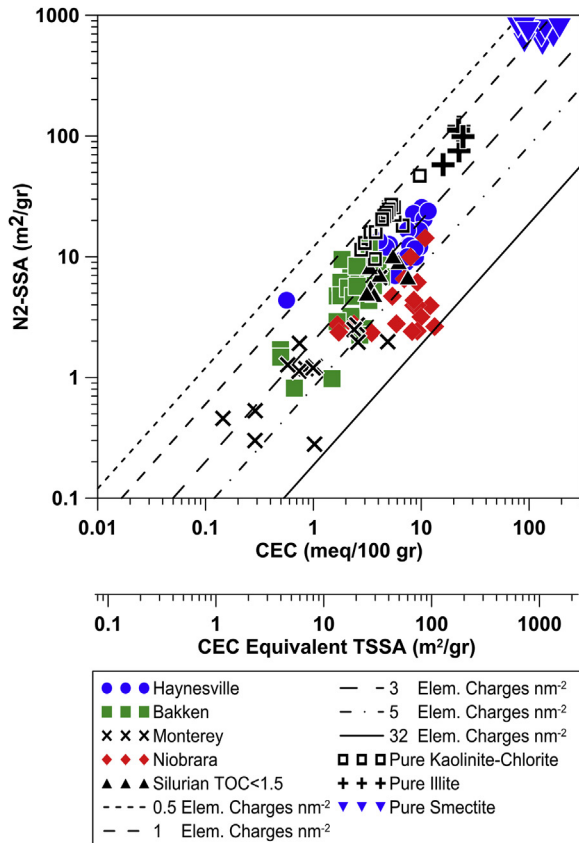


**Fig. 15.** N<sub>2</sub>-SSA correlation with CEC and CEC-TSSA. The charge density for organic rich shales and Bakken in this study is in the 3–5 e/nm<sup>2</sup> range which is equivalent to 0.48–0.80 c/m<sup>2</sup>. Some of the Niobrara samples show a charge density of 32 e/nm<sup>2</sup> which is equivalent to 5.13 c/m<sup>2</sup>. High calculated charge densities are mainly due to underestimated N<sub>2</sub>-SSA. The pure clay data are from [Revil et al. \(2013\)](#).

why nitrogen gas adsorption to characterize surface areas of clay-rich rocks should be taken with great caution, especially when the clay type is smectite.

The iron in the rocks in the form of pyrite can affect the relationship between CEC and SSA. The higher the iron content, the lower the CEC and specific surface area tend to be because of the increased molecular weight ([Derkowski and Bristow, 2012](#)). The iron content, however, cannot explain a dramatic decrease in specific surface area without a decrease in CEC values.

## 6. Conclusions

The CEC and N<sub>2</sub>-SSA were measured for five different oil and gas producing shales ranging from low maturity (oil window Niobrara and Monterey) and high maturity (gas window Haynesville and Silurian) as well as a non-organic rich tight oil formation (Bakken). A wide range of TOC, clay content and type were covered in this study. The following conclusions can be drawn based on the results that were presented in this study:

- It is well-known that clays are the main source of CEC and SSA in different rocks. We showed that this correlation should not be taken for granted in unconventional samples due to the complexity of the mineralogy, geological factors and presence of organic matter with different maturities. The focus of this study was to emphasize that different mud rocks depending on the

mentioned factors might show un-expected correlation between CEC/SSA and clay content.

- CEC values in shales depend on the clay content and type regardless of the TOC and the level of thermal maturity.
- N<sub>2</sub>-SSA is not as sensitive to clay type as CEC and is linearly correlated with mixed layer illite-smectite content.
- OM has more profound effect on N<sub>2</sub>-SSA than CEC. It affects the measured N<sub>2</sub>-SSA in two different ways: (1) Blockage of pores and throats by bituminous kerogen, which limits the accessibility of nitrogen to clay surfaces. This effect was observed in thermally immature (oil window) samples. (2) Development of nano-scale OM-hosted pores with high surface area mostly for thermally mature (gas window) shales.
- The charge density for the samples of this study is overestimated due to underestimation of TSSA by nitrogen adsorption technique.

## Acknowledgements

The authors would like to acknowledge the OCLASSH consortium for funding and support. We also thank Douglas K. McCarty, Leonardo Alcantar Lopez, Rana Elghonimy, Cesar Mapeli and Ashly Burk for help with some of the experiments.

## References

- Archie, G.E., 1942. The electrical resistivity log as an aid in determining some reservoir characteristics. *Pet. Trans. AIME* 146, 54–62.
- Bardon, C., Bieber, M.T., Cuiec, L., Jacquin, C., Courbot, A., Deneuve, G., Simon, J.M., Voirin, J.M., Espy, M., Nectoux, A., Pellerin, A., 1993. Recommandations pour la détermination expérimentale de la capacité d'échange de cations des milieux argileux. *Rev. Inst. Fr. Pét.* 38, 621–626.
- Blum, A.E., Eberl, D.D., 2004. Measurement of clay surface areas by polyvinylpyrrolidone (PVP) sorption and its use for quantifying illite and smectite abundance. *Clays Clay Miner.* 52 (5), 589–602. <http://dx.doi.org/10.1346/CCMN.2004.0520505>.
- Cao, T.T., Song, Z.G., Wang, S.B., Xia, J., 2015. A comparative study of the specific surface area and pore structure of different shales and their kerogens. *Sci. China Earth Sci.* 58 (4), 510–522. <http://dx.doi.org/10.1007/s11430-014-5021-2>.
- Chiou, C.T., Rutherford, D.W., Manes, M., 1993. Sorption of nitrogen and ethylene glycol monoethyl ether (EGME) vapors on some soils, clays, and mineral oxides and determination of sample surface areas by use of sorption data. *Environ. Sci. Technol.* 27 (8), 1587–1594. <http://dx.doi.org/10.1021/es00045a014>.
- Clavier, C., Coates, G., Dumanoir, J., 1984. Theoretical and experimental bases for the dual-water model for interpretation of shaly sands. *Soc. Pet. Eng. J.* 24 (2), 3–20.
- Derkowski, A., Bristow, T.F., 2012. On the problems of total specific surface area and cation exchange capacity measurements in organic-rich sedimentary rocks. *Clays Clay Miner.* 60 (4), 348–362. <http://dx.doi.org/10.1346/CCMN.2012.0600402>.
- Ding, F., Cai, J.G., Song, M.S., Yuan, P., 2013. The relationship between organic matter and specific surface area in <2 μm Clay size fraction of muddy source rock. *Sci. China Earth Sci.* 56 (8), 1343–1349. <http://dx.doi.org/10.1007/s11430-013-4606-5>.
- Ellis, D.W., 1987. *Well Logging for Earth Scientists*. Elsevier, New York, 572 pp.
- Godinez, L.J., 2013. Control Factors for Fluid Saturation and Pore Size Distributions Based on Gas Adsorption, CEC and 2D Dielectric Microscopy: a Case Study of the Quartz Phase Porcelanites in the Miocene Monterey Formation (M.Sc. thesis). Colorado School of Mines.
- Heister, K., 2014. The measurement of the specific surface area of soils by gas and polar liquid adsorption methods-limitations and potentials. *Geoderma* 2016, 75–87. <http://dx.doi.org/10.1016/j.geoderma.2013.10.015>.
- Keil, R.G., Montluçon, D.B., Fredrick, G., Prah, F.G., Hedges, J.L., 1994. Sorptive preservation of labile organic matter in marine sediments. *Nature* 370, 549–552. <http://dx.doi.org/10.1038/370549a0>.
- Kennedy, M.J., Wagner, T., 2011. Clay mineral continental amplifier for marine carbon sequestration in a greenhouse ocean. *Proc. Natl. Acad. Sci. U. S. A.* 108 (24), 9776–9781. <http://dx.doi.org/10.1073/pnas.1018670108>.
- Kennedy, M.J., Pevear, D.R., Hill, R.J., 2002. Mineral surface control of organic carbon in black shale. *Science* 295 (5555), 657–660. <http://dx.doi.org/10.1126/science.1066611>.
- Kuila, U., 2013. *Measurement and Interpretation of Porosity and Pore-size Distribution in Mudrocks: the Hole Story of Shales* (Ph.D. thesis). Colorado School of Mines.
- Kuila, U., Prasad, M., 2013. Specific surface area and pore-size distribution in clays and shales. *Geophys. Prospect.* 61, 341–362. <http://dx.doi.org/10.1111/1365-2478.12028>.
- Kuila, U., Prasad, M., Derkowski, A., McCarty, D., 2012. Compositional controls on

- mudrock pore-size distribution: an example from Niobrara formation. In: SPE Annual Technical Conference and Exhibition. <http://dx.doi.org/10.2118/160141-MS>. SPE Paper 160141.
- Kuila, U., McCarty, D.K., Derkowski, A., Fischer, T.B., Topór, T., Prasad, M., 2014. Nano-scale texture and porosity of organic matter and clay minerals in organic-rich mudrocks. *J. Fuel* 135, 359–373. <http://dx.doi.org/10.1016/j.fuel.2014.06.036>.
- Lang, F., Kaupenjohann, M., 2003. Immobilisation of molybdate by iron oxides: effects of organic coatings. *Geoderma* 113 (1–2), 31–46. [http://dx.doi.org/10.1016/S0016-7061\(02\)00314-2](http://dx.doi.org/10.1016/S0016-7061(02)00314-2).
- Loucks, R.G., Reed, R.M., Ruppel, S.C., Hammes, U., 2012. Spectrum of pore types and networks in mudrocks and a descriptive classification for matrix-related mudrock pores. *AAPG Bull.* 96 (6), 1071–1098. <http://dx.doi.org/10.1306/08171111061>.
- Maček, M., Mauko, A., Mladenović, A., Majes, B., Petkovšek, A., 2013. A comparison of methods used to characterize the soil specific surface area of clays. *Appl. Clay Sci.* 83–84, 144–152. <http://dx.doi.org/10.1016/j.clay.2013.08.026>.
- Mayer, L.M., Xing, B., 2001. Organic matter–surface relationships in acid soils. *Soil Sci. Soc. Am. J.* 65 (1), 250–258. <http://dx.doi.org/10.2136/sssaj2001.651250x>.
- Mikutta, C., Lang, F., Kaupenjohann, M., 2004. Soil organic matter clogs mineral pores: evidence from <sup>1</sup>H-NMR and N<sub>2</sub> adsorption. *Soil Sci. Soc. Am. J.* 68, 1853–1862. <http://dx.doi.org/10.2136/sssaj2004.1853>.
- Milliken, K.L., Rudnicki, M., Awwiller, D.N., Zhang, T., 2013. Organic matter-hosted pore system, marcellus formation (Devonian), Pennsylvania. *AAPG Bull.* 97 (2), 177–200. <http://dx.doi.org/10.1306/07231212048>.
- Passey, Q.R., Bohacs, K.M., Esch, W.L., Klimentidis, R., Sinha, S., 2010. From oil-prone source rock to gas-producing shale reservoir—geologic and petrophysical characterization of unconventional shale-gas reservoirs. In: International Oil and Gas Conference and Exhibition. <http://dx.doi.org/10.2118/131350-MS>. SPE Paper 131350.
- Patchett, J.G., 1975. An investigation of shale conductivity. In: SPWLA 16th Annual Logging Symposium, 4–7 June, New Orleans, Louisiana.
- Peinemann, N., Amiotti, N.M., Zalba, P., Villamil, M.B., 1999. Effect of clay minerals and organic matter on the cation exchange capacity of silt fractions. *J. Plant Nutr. Soil Sci.* 163 (1), 47–52. [http://dx.doi.org/10.1002/\(SICI\)1522-2624\(200002\)163:1<47::AID-JPLN47>3.0.CO;2-A](http://dx.doi.org/10.1002/(SICI)1522-2624(200002)163:1<47::AID-JPLN47>3.0.CO;2-A).
- Pezard, P.A., 1990. Electrical properties of mid-ocean ridge basalt and implications for the structure of the upper oceanic crust in hole 504B. *J. Geophys. Res. Solid Earth* 95 (B6), 9237–9264. <http://dx.doi.org/10.1029/JB095iB06p09237>.
- Revil, A., Cathles III, L.M., Losh, S., Nunn, J.A., 1998. Electrical conductivity in shaly sands with geophysical applications. *J. Geophys. Res.* 103 (B10), 23925–23936. <http://dx.doi.org/10.1029/98JB02125>.
- Revil, A., Eppheimer, J.D., Skold, M., Karaoulis, M., Godinez, L., Prasad, M., 2013. Low-frequency complex conductivity of sandy and clayey materials. *J. Colloid Interface Sci.* 398, 193–209. <http://dx.doi.org/10.1016/j.jcis.2013.01.015>.
- Ridge, M.J., 1983. A combustion method to measure the cation exchange capacity of clay minerals. *Log. Anal.* 24 (3), 6–11.
- Rivera, S., Saidian, M., Godinez, L.J., Prasad, M., 2014. Effect of mineralogy on NMR, sonic, and resistivity: a case study of the Monterey formation. In: Unconventional Resources Technology Conference, August 25–27, Denver, CO, URTEC 1922872. <http://dx.doi.org/10.15530/urtec-2014-1922872>.
- Saidian, M., Prasad, M., 2015. Effect of mineralogy on nuclear magnetic resonance surface relaxivity: a case study of Middle Bakken and Three Forks formations. In: SPE Annual Technical Conference and Exhibition, Houston, Texas, USA, 28–30 September, SPE-175052-MS.
- Saidian, M., Kuila, U., Prasad, M., Alcantar-Lopez, L., Rivera, S., Godinez, L.J., 2016. A comparison of measurement techniques for porosity and pore size distribution in mudrocks: a case study of Haynesville, Niobrara, Monterey and Eastern European Silurian formations. *AAPG Mem.* 112. Imaging Unconventional Pore Systems, (in press).
- Sing, K.S.W., Everett, D.H., Haul, R.A.W., Moscou, L., Pierotti, R.A., Rouquerol, J., Siemieniowska, T., 1985. Reporting physisorption data for gas/solid systems, IUPAC commission on colloid and surface chemistry including catalysis, *Pure Appl. Chem.*, v. 57, p. 603.
- Środoń, J., 2009. Quantification of illite and smectite and their layer charges in sandstones and shales from shallow burial depth. *Clay Miner.* 44 (4), 421–434. <http://dx.doi.org/10.1180/claymin.2009.044.4.421>.
- Thomas, E. C., 1976. Determination of Q<sub>v</sub> from membrane potential measurements on shaly sands. *J. Pet. Technol.*, v. 28, n. 9, p. 1087–1096, doi: 10.2118/5505-PA.
- Van Olphen, H., Fripiat, J.J., 1979. *Data Handbook for Clay Minerals and Other Non-metallic Minerals*. Pergamon Press, Oxford, England, 346 pp.
- Waxman, M.H., Smits, L.J.M., 1968. Electrical conductivities in oil-bearing shaly sands. *Soc. Pet. Eng. J.* 107–122.
- Wiklander, L., 1964. In: Bear, F.E. (Ed.), *Chemistry of the Soil*, second ed. Van Nostrand Reinhold, New York.
- Woodruff, W.F., Revil, A., 2011. CEC-normalized clay-water sorption isotherm. *Water Resour. Res.* 47 (11), W11502. <http://dx.doi.org/10.1029/2011WR010919>.
- Zargari, S., Prasad, M., Kenechukwu, M.C., Mattson, E.D., 2013. Organic maturity, elastic properties, and textural characteristics of self-resourcing reservoirs. *Geophysics* 78 (4), D223–D235. <http://dx.doi.org/10.1190/geo2012-0431.1>.
- Zargari, S., Canter, K.L., Prasad, M., 2015. Porosity evolution in oil-prone source rocks. *Fuel* 153, 110–117. <http://dx.doi.org/10.1016/j.fuel.2015.02.072>.
- Zhu, X., Cai, J., Wang, X., Zhang, J., Xu, J., 2014. Effects of organic components on the relationships between specific surface areas and organic matter in mudrocks. *Int. J. Coal Geol.* 133, 24–34. <http://dx.doi.org/10.1016/j.coal.2014.08.009>.